marily to the blackbody radiation emitted by the clouds and surface, which is isotropic. At these wavelengths, clouds more than about 300 m thick emit as blackbodies (*6*), and therefore the infrared channel yields an estimate of the cloud-top temperature. If the vertical temperature profile is known, the height of the cloud top can be determined.

In Fig. 1 the threshold defining cloud areas is somewhat arbitrarily set at $-10°C$ for the cloud-top temperature. If the threshold is raised too much, we risk including parts of the ocean in our cloud areas. If it is lowered too much, we obtain very few regions of appreciable extent. The choice of $-10°C$ is a compromise between these extremes. Some experimentation with different thresholds ($-15°$ and $-5°C$) yielded similar results. Changing the threshold decreases or increases the size of the clouds for colder or warmer thresholds, respectively. However, the perimeters change in such a way that the points remain on the line shown in Fig. 1.

Physically, the rain and cloud fields are closely related in the tropics, since both occur in regions of convective updraft, which causes the moist warm surface air to rise, cool by adiabatic expansion, and form clouds and rain in the resulting condensation processes. Because of the relatively short time scale of these processes, much of these clouds, even at $-20°$ or $-30°C$, is supercooled water rather than ice. The cloud area delineated by the $-10°C$ threshold thus contains regions of both cumulus and cirrus clouds (composed mainly of supercooled droplets and ice particles, respectively).

For convenience, GOES pictures of the Indian Ocean region sampled at resolutions of 4.8 and 19.2 km were used. To avoid effects of varying picture element size, primarily due to the earth's curvature, only data in the relatively undistorted region between 20°N and 20°S and within ± 30° of longitude of the subsatellite point were used. Because effects due to the earth's curvature are similar for both area and perimeter, the $A/P$ ratio is affected only to second order. Therefore image distortion should not yield a systematic effect in Fig. 1, even for the largest cloud examined, which extended over 3000 km from Africa to south of India (with an area of $\sim 1.2 \times 10^6$ km$^2$).

The most striking aspect of Fig. 1 is the absence of any apparent bend or kink over the range of more than six orders of magnitude in area. This is important because the evidence to date, based largely on Fourier spectra of wind variations, has been inconclusive about the existence of length scales, particularly in the range 1 to 1000 km. Theoretically, such a length scale might arise because of the gradual transition from a three-dimensional turbulent regime at small scales to a two-dimensional regime at a scale of hundreds of kilometers, where the atmosphere would appear thin (the scale height of the atmosphere is $\sim$ 10 km). Indeed, early investigations pointed to the existence of a "mesoscale gap" in wind spectra [for instance (*7*)]. However, later research showed this situation to be the exception rather than the rule (*8*) and indicated no break in the spectrum for distances up to at least 1000 km. Experiments with high-altitude balloons also failed to show evidence of a length scale in the range 100 to 1000 km (*9*), and clear air Doppler radar wind measurements showed no length scales in the range 4 to 400 km (*10*). Recently, Doppler wind spectra in rainy regions failed to show any evidence of length scales in the range 1.6 to 25 km (*11*).

Although higher resolution radar or satellite data are needed to extend Fig. 1 in the direction of smaller $A$, other experiments, such as aircraft measurements of wind spectra (*12*), found no evidence of length scales down to 10 m. Indeed, as Richardson's (*13*) famous atmospheric diffusion experiment suggested, the range of scaleless behavior may continue down to distances of centimeters, where viscosity becomes important. If Richardson was right, then a fractal model of the atmosphere may be appropriate over a large fraction of the range of meteorologically significant distances.

Finally, it is interesting to speculate on the empirical value of $D$ obtained from Fig. 1. The value 1.35 is so close to the value 4/3 (that of turbulent isobars) that some fairly straightforward connection may exist. An understanding of the physical origins of this value could therefore be important.

S. LOVEJOY

*Centre de Recherches Atmosphériques de Magny les Hameaux, 78470 Saint Remy les Chevreuse, France*

**References and Notes**

1. B. Mandelbrot, *Fractals* (Freeman, San Francisco, 1977).
2. L. F. Richardson, *Proc. R. Soc. London Ser. A* **110**, 709 (1926).
3. G. K. Batchelor, *The Theory of Homogeneous Turbulence* (Cambridge Univ. Press, New York, 1953).
4. S. Lovejoy, *Preprint Volume, 20th Conference on Radar Meteorology* (American Meteorological Society, Boston, 1981), p. 476.
5. The intrinsic resolution of the satellite sensor is 6.4 km, but the data available on magnetic tape were sampled at 4.8 km to be compatible with the data from the higher resolution visible sensor.
6. F. Mosher, thesis, University of Wisconsin, Madison (1979).
7. J. Van der Hoven, *J. Meteorol.* **14**, 160 (1957).
8. N. K. Vinnichenko, *Tellus* **22**, 158 (1970).
9. P. Morel and M. Larcheveque, *J. Appl. Meteorol.* **31**, 2189 (1974).
10. K. S. Gage, *J. Atmos. Sci.* **36**, 1950 (1979).
11. M. Gilet, S. Nicoloff, V. Klaus, C. Gaillard, *Preprint Volume, 19th Conference on Radar Meteorology* (American Meteorological Society, Boston, 1980), p. 30.
12. J. I. MacPherson and G. A. Isaac, *J. Appl. Meteorol.* **16**, 81 (1977).
13. L. F. Richardson, *Beitr. Phys. Freien Atmos.* **15**, 24 (1929).
14. I thank B. Mandelbrot, G. L. Austin, J. C. André, D. Schertzer, M. Gilet, and U. Phadke for helpful discussions and comments.

4 August 1981; revised 30 December 1981

# Maceral, Total Organic Carbon, and Palynological Analyses of Ross Ice Shelf Project Site J9 Cores

Abstract. *Analyses of macerals and total organic carbon indicate that the low organic content of core sediments from Ross Ice Shelf Project site J9 has been selectively reduced further, probably by postdepositional submarine oxidation. Palynological analysis revealed a reworked Paleogene dinocyst flora of low diversity (the transantarctic flora). This constitutes the most southerly dinocyst flora reported thus far. The antarctic distribution of the transantarctic flora supports the existence of a transantarctic strait during the Paleogene. The J9 sporomorph assemblage also is reworked and Paleogene in age.*

Gravity cores recovered by the Ross Ice Shelf Project from site J9 (82°22′S, 168°38′W) have provided the first bottom sediments from beneath the southern Ross Ice Shelf for scientific research (*1*). Maceral and total organic carbon (TOC) analyses were conducted on core samples to document the types and distribution of macerals present, to determine the TOC profiles, and to study the effects of reported submarine oxidation on the maceral and TOC contents. A preliminary palynological investigation also has been conducted on a low-diversity palynoflora observed during maceral analysis (*2*).

Previous sedimentological investigations have demonstrated the presence of two lithologic units in each core (*1*). The lighter colored upper unit (unit 2) is an


0036-8075/82/0409-0187$01.00/0 

Table 1. Palynomorphs recovered from Ross Ice Shelf Project site J9 cores. Age ranges are shown to the right of taxa identified to the species level.

| Microplankton | Age | Pollen and spores | Age |
|---|---|---|---|
| Dinophyceae | | Angiosperms | |
| *Apectodinium homomorphum* (Deflandre and Cookson) Lentin and Williams | Upper Paleocene to Middle Oligocene | *Beaupreaidites* cf. *B. elegansiformis* Cookson | |
| *Cleistosphaeridium* spp. | | *Nothofagidites flemingii* (Couper) Potonie | Middle Paleocene to Upper Eocene |
| *Deflandrea antarctica* Wilson | Eocene | *Nothofagidites* spp. | |
| *Hystrichosphaeridium* sp. | | *Tricolpites* spp. | |
| *Pareodinia* sp. | | | |
| *Spinidinium macmurdoense* (Wilson) Lentin and Williams | Paleogene | *Triorites fragilis* Couper | ?Upper Senonian to Middle Eocene |
| *Spiniferites* sp. | | Unidentified angiosperms | |
| *Vozzhennikovia rotunda* (Wilson) Lentin and Williams | Early Eocene to Oligocene | Gymnosperms | |
| | | *Podocarpidites* spp. | |
| *Vozzhennikovia apertura* (Wilson) Lentin and Williams | Eocene to Early Oligocene | *Phyllocladidites mawsonii* Cookson | Turonian to Miocene |
| | | *Microcachryidites antarcticus* Cookson | Jurassic to Miocene |
| Unidentified dinocysts | | Unidentified gymnosperms | |
| Acritarcha | | Spores | |
| *Cymatiosphaera* sp. | | *Lycopodiumsporites* sp. | |
| Unidentified acritarch | | *Laevigatosporites* sp. | |
| *Tasmanites* sp. | | Unidentified fungal spores | |
| Microforaminifera | | | |

oxidized alteration product of sediments that probably were identical to those of the lower unit (unit 1) at the time of sedimentation. A yellow-brown, iron-rich boundary layer separating the two units marks the depth of penetration, below the sea floor, of the advancing oxidation front.

The age of the cored sediments is controversial. Benthonic foraminifera suggest an early to middle Miocene age (*1*), whereas silicoflagellate studies indicate a Miocene (*3*) or middle Miocene age (*4*). Diatom-based age determinations of middle Miocene (*5*), late middle Miocene (*6*), and late Pleistocene (*7*) have been proposed. Although these age determinations differ with respect to epochal assignment, they are all post-Paleogene. Concentrations of cosmogenic $^{10}Be$ in the core sediments indicate that they are pre-Quaternary and that they have not been mixed for millions of years (*8*). Overall, the evidence indicates a middle Miocene age for the cores.

Sixteen samples were selected from 6 of the 11 cores collected during the 1977–1978 austral summer field season. The samples can be treated as components of a single composite core because the cores were collected within 15 m of each other, are all less than 1 m long, and are lithologically similar.

Maceral analysis is the microscopic study of particulate, acid-resistant organic matter (macerals) in sedimentary deposits (*9*). Maceral and TOC sample preparation and analyses were conducted according to procedures previously reported (*9*). Macerals were counted and categorized according to type, preservation, and color (an index of thermal alteration). The types recognized include phytoclasts (terrestrial plant fragments, spores, pollen), protistoclasts (acritarchs, dinocysts, foraminifera linings), scleratoclasts (fungal spores, hyphae, and fruiting bodies), and amorphous indeterminate (AI) macerals. The latter are organic matter initially unstructured or

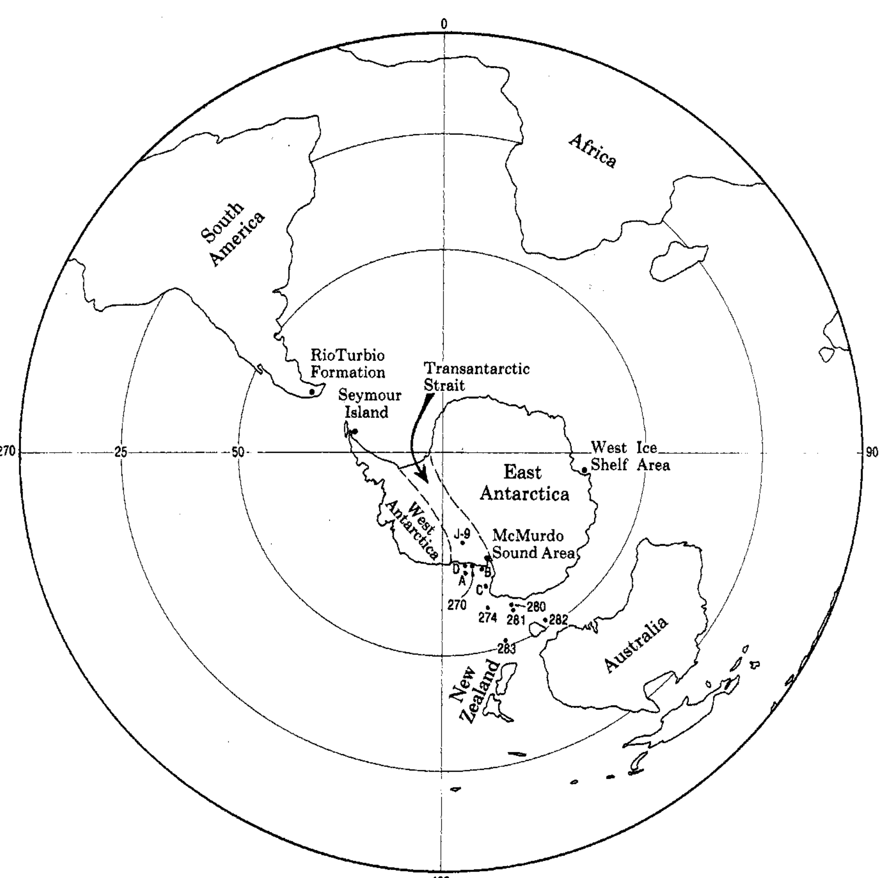


Fig. 1. Map showing the location of sites where components of the transantarctic flora have been reported. The relative positions of the continents are those of the Late Eocene. Deep Sea Drilling Project localities include sites 270, 274, and 280 through 283 (*10, 11*). Letters *A*, *B*, *C*, and *D* represent Wilson's (*13*) grab sample stations A452, A459, A461, and A466, respectively. The trend of the hypothesized transantarctic strait is shown by dashed lines. The map was adapted from Firstbrook *et al.* (*22*).

so completely degraded as to defy assignation to any other maceral category.

Phytoclasts are the dominant macerals in the cores, followed, in order of decreasing abundance, by protistoclasts, scleratoclasts, and AI macerals. The maceral and TOC data for each unit of the composite core were combined into two groups (representing units 1 and 2) and statistically tested for differences. A Student's $t$-test of the maceral data revealed a highly significant difference in the mean content of AI macerals between unit 1 (13 percent) and unit 2 (2 percent) ($P < .01$). The mean TOC content was also significantly higher in unit 1 (0.43 percent) than in unit 2 (0.29 percent) ($P < .01$).

Light and dark macerals occur together throughout the cores. This indicates mixing of reworked, thermally mature macerals and less thermally mature macerals during middle Miocene deposition of the cored sediments. There was no indication of postdepositional thermal alteration of the organic matter.

We conclude (i) that the original sediments (organic and inorganic) were essentially homogeneous, (ii) that postdepositional alteration created two distinct lithologies (units 1 and 2), (iii) that unit 2 contains significantly lower AI maceral and TOC contents, (iv) that the selective removal of AI macerals resulted in the lower TOC values in unit 2, and (v) that the low incidence of biologically attacked macerals suggests chemical postdepositional destruction of AI macerals in unit 2, probably by submarine oxidation.

Dinocysts, acritarchs, and sporomorphs are present throughout the cored sequence (Table 1). Chlorophyceae and microforaminifera, although rare, are also present. The dinocyst flora reported here includes *Deflandrea antarctica* Wilson, *Spinidinium macmurdoense* (Wilson) Lentin and Williams, *Vozzhennikovia rotunda* (Wilson) Lentin and Williams, and *V. apertura* (Wilson) Lentin and Williams. These species belong to a microplankton flora characteristic of high southern latitudes (*10, 11*), referred to here as the transantarctic flora. Kemp (*10*) considered this microplankton flora to be of late Eocene age. Haskell and Wilson (*11*) suggested an earlier Tertiary age.

Components of this flora have been reported from the West Ice Shelf area (*12*), Deep Sea Drilling Project sites 270, 274, and 280 to 283 (*10, 11*), the northern Ross Sea (*13*), the McMurdo Sound area (*14*), Seymour Island (*15*), and southern Argentina (*16*) (Fig. 1).

The late Paleogene dinocyst assemblages are accompanied by sporomorph assemblages, which generally include *Nothofagidites* species, *Podocarpidites* species, *Microcachryidites antarcticus*, and *Phyllocladidites mawsonii*. The widespread co-occurrence of the sporomorph and microplankton assemblages in reworked and in situ deposits of the high southern latitudes suggests that both assemblages are late Paleogene in age. Thus, the palynomorph assemblages in the J9 cores are not coeval with the accompanying Neogene diatom assemblages, as stated by Brady and Martin (*6*). Rather, the palynomorphs indicate that extensive reworking occurred contemporaneously with Neogene sedimentation in the J9 area. This contention is supported by the presence of reworked Upper Cretaceous foraminifera in the Ross Ice Shelf Project cores (*17*).

The spore and pollen species observed by Brady and Martin (*6*) led them to conclude that a continental vegetation of low diversity existed in parts of Antarctica during the middle Miocene. However, the reworked nature of the palynomorph assemblage discussed here indicates that their paleoenvironmental interpretation is based on mixed fossil material (that is, late Paleogene palynomorphs and Neogene diatoms).

The reworked Paleogene palynomorph assemblages reported from the Ross sector [sensu Webb (*18*)] probably have a common provenance. The only known outcrops of Paleogene marine sediments in Antarctica occur on Seymour Island, 3000 km northeast of the Ross Sea (*19*). It is unlikely that this is the source area, since it is located in a different drainage basin (*20*). There is very little evidence suggesting that the J9 sediments were derived from East Antarctica or that they crop out elsewhere on the floor of the Ross Sea. Webb and co-workers (*1*) suggested that at least part of the J9 sediments were derived from the Whitmore Mountains in Marie Byrd Land. This contention is supported by present-day movement of ice into the Ross Sea from the east (*20*). Presumably, ice flow patterns were similar during the time of J9 sediment deposition. It seems likely that the Paleogene source beds, if they still exist, lie under the west antarctic ice sheet.

This investigation provides data important for late Paleogene geographic reconstructions of Antarctica. During the late Paleogene, the transantarctic flora extended from the present-day West Ice Shelf area eastward between Australia and Antarctica, into the Ross Sea, across West Antarctica, and into southernmost South America (Fig. 1). This distribution supports the concept of a transantarctic strait connecting the Ross and Weddell seas (*18*) prior to the opening of the Drake Passage. The strait would have facilitated dispersal of the transantarctic flora, perhaps by means of a current circulating around East Antarctica (*18*). The coalescence of the east and west antarctic ice sheets closed the strait, presumably soon after the opening of the Drake Passage and the attendant thermal isolation of Antarctica in the Late Oligocene or Early Miocene (*21*).

JOHN H. WRENN*
*Department of Geology, Louisiana State University, Baton Rouge 70803*
SCOTT W. BECKMAN†
*Department of Marine Sciences, Louisiana State University*

**References and Notes**

1. P. N. Webb, *Ross Ice Shelf Proj. Tech. Rep. 78-1* (1978); *Ross Ice Shelf Proj. Tech. Rep. 79-1* (1979); ______, T. E. Ronan, Jr., J. H. Lipps, T. E. DeLaca, *Science* **203**, 435 (1979).
2. J. H. Wrenn, *Antarct. J. U.S.*, in press.
3. H. Y. Ling and R. J. White, *ibid.* **14**, 126 (1979).
4. R. J. White, thesis, Northern Illinois University, DeKalb (1980).
5. H. T. Brady, *Antarct. J. U.S.* **12**, 123 (1978).
6. ______ and H. Martin, *Science* **203**, 437 (1979).
7. D. A. Kellogg and T. B. Kellogg, *Antarct. J. U.S.* **15**, 61 (1980).
8. F. Yiou and G. M. Raisbeck, *Eos* **62**, 297 (1981).
9. J. H. Wrenn and S. W. Beckman, *Antarct. Res. Ser.* **33**, 391 (1981).
10. E. M. Kemp, *Init. Rep. Deep Sea Drilling Proj.* **28**, 599 (1975).
11. T. R. Haskell and G. J. Wilson, *ibid.* **29**, 723 (1975).
12. E. M. Kemp, *Mar. Geol.* **13**, 145 (1972).
13. G. J. Wilson, *N. Z. J. Mar. Freshwater Res.* **2**, 381 (1968).
14. D. J. McIntyre and G. J. Wilson, *N. Z. J. Bot.* **4**, 315 (1966); G. J. Wilson, *ibid.* **5**, 57 (1967).
15. S. A. Hall, *Nature (London)* **267**, 239 (1977); J. H. Wrenn, in preparation.
16. S. Archangelsky, *Ameghiniana* **6**, 181 (1969).
17. P. N. Webb, *J. R. Soc. N.Z.* **11** (No. 4) (1981).
18. ______, *Dry Valley Drilling Project (DVDP) Seminar III* (National Institute of Polar Research, Tokyo, 1978), Bulletin 8; in *Proceedings of the Seminar III on Dry Valley Drilling Project, 1978*, T. Nagata, Ed. (National Institute of Polar Research, Tokyo, 1979), p. 206.
19. D. H. Elliot, C. Rinaldi, W. J. Zinsmeister, T. A. Trautman, W. A. Bryant, R. Del Valle, *Antarct. J. U.S.* **10**, 182 (1975).
20. H. G. Goodell, in *Antarctic Map Folio Series, Folio 17*, V. C. Bushnell, Ed. (American Geographical Society, New York, 1973), p. 1.
21. P. F. Barker and J. Burrell, *Mar. Geol.* **25**, 15 (1977).
22. P. L. Firstbrook, B. M. Funnell, A. M. Hurley, A. G. Smith, *Paleoceanic Reconstructions, 160-0 Ma* (National Ocean Sediment Coring Project, La Jolla, Calif., 1979), p. 41.
23. We thank the Division of Polar Programs at the National Science Foundation for making the core samples available; the Department of Geology at Louisiana State University for support; and D. S. Cassidy for his meticulous sampling of the J9 cores. We also thank R. W. Aurisano, J. A. Babcock, D. N. Beju, E. J. Kidson, and P. N. Webb for critically reading the manuscript. Technical support during manuscript preparation by the Amoco Production Company Research Center, Tulsa, Okla., is gratefully acknowledged.

* Present address: Amoco Production Company Research Center, P.O. Box 591, Tulsa, Okla. 74102.
† Present address: Phillips Petroleum Company, Research and Development, Bartlesville, Okla. 74004.

29 October 1981; revised 30 December 1981